

Research

A low dose of curcumin-PDA nanoparticles improves viability and proliferation in endoneurial fibroblasts and Schwann cell cultures

Lucia Vázquez Alberdi^{1,2} · Marcela Martínez-Busi³ · Eloisa Arrarte⁴ · Carolina Echeverry⁵ · Miguel Calero⁶ · Alejandra Kun^{1,7}

Received: 20 December 2023 / Accepted: 23 April 2024

Published online: 07 May 2024

© The Author(s) 2024 [OPEN](#)

Abstract

Curcumin is a polyphenol extracted from *Curcuma longa*'s roots. Low doses of curcumin are related to anti-inflammatory, antioxidant, and neuroprotective effects, while high doses are used for their lethality. This diversity of behaviors allows us to understand curcumin as a compound with hormetic action. Due to its strongly hydrophobic character, curcumin is often solubilized in organic compounds. In this way, we have recently reported the undesirable and occasionally irreversible effects of alcohol and DMSO on the viability of primary Schwann cell cultures. In this scenario, the use of nanoparticles as delivery systems has become a successful alternative strategy for these compounds. In the present work, we describe the structure of Polydopamine (PDA) nanoparticles, loaded with a low dose of curcumin (Curc-PDA) without the use of additional organic solvents. We analyzed the curcumin released, and we found two different forms of curcumin. Small increased cell viability and proliferation were observed in endoneurial fibroblast and Schwann cell primary cultures when Curc-PDA was steadily supplied for 5 days. The increased bioavailability of this natural compound and the impact on cells in culture not only confirm the properties of curcumin at very low doses but also provide a glimpse of a possible therapeutic alternative for PNS conditions in which SCs are involved.

Keywords Curcumin · Polydopamine-nanoparticles · Hormesis · Viability · Proliferation

1 Introduction

Curcumin is a polyphenol extracted from the roots of the *Curcuma longa* plant, native to India [1–4]. It is a yellow-orange solid with diverse applications, with a broad spectrum of action depending on its concentration and the administration time [5–12]. It has been reported that low doses of curcumin are related to anti-inflammatory [13, 14], antioxidant [9, 15–17], and neuroprotective effects [10, 11, 18, 19]; whereas, at high concentrations, it has lethal

Supplementary Information The online version contains supplementary material available at <https://doi.org/10.1186/s11671-024-04023-7>.

✉ Lucia Vázquez Alberdi, lvazquez@iibce.edu.uy; ✉ Alejandra Kun, akun@fcien.edu.uy | ¹Laboratorio de Biología Celular del Sistema Nervioso Periférico, Departamento de Proteínas y Ácidos Nucleicos, Instituto de Investigaciones Biológicas Clemente Estable, Montevideo, Uruguay. ²Laboratorio de Acústica, Facultad de Ciencias, Instituto de Física, UdelaR, Montevideo, Uruguay. ³Plataforma Química Analítica, Instituto de Investigaciones Biológicas Clemente Estable, Montevideo, Uruguay. ⁴Área Físicoquímica, Facultad de Química, UdelaR, Montevideo, Uruguay. ⁵Departamento de Neurobiología y Neuropatología, Instituto de Investigaciones Biológicas Clemente Estable, Montevideo, Uruguay. ⁶Unidad de Encefalopatías Espongiformes, UFIEC, CIBERNED, Instituto de Salud Carlos III, Madrid, Spain. ⁷Sección Bioquímica, Facultad de Ciencias, Universidad de La República, Montevideo, Uruguay.



effects, is used as a potent anti-tumor agent [5–8, 20, 21]. This diversity of behaviors allows us to understand curcumin as a hormetic compound. Thus, at low doses, it has cellular effects that promote cell development, while at high doses it promotes cell death [22–24].

Due to its hydrophobic character, curcumin needs to be solubilized in organic solvents, the most conventionally used being ethanol and dimethyl sulfoxide (DMSO) [20, 21, 25–28]. Unfortunately, these vehicles present effects by themselves (especially visible at prolonged exposure times), more or less detectable depending on the biological models used [29–32]. Recently, we have reported effects on the viability and proliferation of primary Schwann cell cultures of both ethanol and DMSO, irreversible in a pathological context, after 6 days of treatment [30].

Given the great versatility of curcumin, the limitations of its conventional vehicles, and its low bioavailability, several strategies have emerged to improve its delivery. The use of cyclodextrin/cellulose nanocrystals coated with curcumin [33, 34], curcumin in polyethylene glycol [35, 36], nanosuspension in tween-80 [37], in chitosan/aloe film [38], conjugated to polyacetal [39], constitute some different strategies reported to the vehicle this compound, although there are many others [40–42].

Among other alternative approaches, the use of nanoparticles as delivery systems is a successful strategy [43–45]. Recently, polydopamine (PDA) nanoparticles have been used not only as coatings and surface functionalization [46, 47] but also as vehicles of different compounds [48–52]. Some studies have used PDA to vehicle curcumin with some differences. Pan et al. 2020 created carrier-free curcumin nanoparticles of different concentrations between 4 and 50 µg/ml (approximately between 11 µM and 136 µM), which they subsequently coated with PDA, demonstrating that these curcumin-loaded nanoparticles are stable structures, with curcumin release dependent on pH variations [49]. In 2021, Su et al. produced PDA nanoparticles, and then exposed them to curcumin (around 1.13 mM curcumin), demonstrating their antioxidant and antibacterial properties in yeast cultures [50]. Zhao et al., 2022 use PDA nanoparticles coating curcumin loaded with poly L-lactic acid for chemo-photo thermal therapy of osteosarcoma. The work demonstrates that by thermo-activation of nanoparticles loaded with approximately 1 mg/ml curcumin (\approx 2.72 mM), their release in human osteosarcoma cultures (MG-63) is possible, depending on the pH of the intracellular medium [51]. Recently, Lei et al., 2023 coated a rabies virus glycoprotein (RVG29 peptide) to PDA nanoparticles with 0.3 mmol curcumin previously dissolved in PEG and DMSO (approximately 2.24 mM), to target the nanoparticles to the murine brain. The work explores the antiaggregatory effects of curcumin on α -synuclein in different experimental models (Balb/c mice, *C. elegans*, and PC12 cell culture). The results further demonstrate a decrease in oxidative stress levels and apoptosis upon delivery of curcumin through these nanoparticles [52]. The literature thus points to the sensitivity and dependence of curcumin release from PDA nanoparticles in response to the pH of the medium. The different effects of curcumin on the dose used, evidence its hormetic action, especially when considering the use of these nanoparticles at the biological level [50–52].

Primary culture approaches can be used to understand metabolic responses during specific stimuli or insults. In the peripheral nerve fiber, in addition to neurons, Schwann cells (SC) and endoneurial fibroblasts (EFB) are present. Establishing primary cultures of SCs and EFBs allows us to understand the metabolic responses of in vitro proliferation. In the healthy nerve fiber, SCs and EFBs show a very low proliferative rate, mainly activating it in response to damage [53, 54]. However, under neurodegenerative conditions, proliferation is a frequent event in response to punctate or permanent injury [16, 33].

In the present work, we propose a new fabrication and loading protocol for Curc-PDA, without using organic solvent to load curcumin into PDA. This protocol incorporates a key dialysis step to eliminate possible pH variations outside the physiological range. We describe the structure of PDA nanoparticles, loaded or not with curcumin, by Transmission/Scanning Electron Microscopy (TEM and SEM) and Diffraction Light Scattering (DLS). We analyze their loading and unloading dynamics with curcumin, characterizing the released compounds by Ultra-High-Pressure-Liquid Chromatography with a Mass-Spectrometry (UHPLC-MS). Finally, we tested the safety of PDA as a vehicle (without curcumin) and the functional dynamics of nanoparticles loaded with low doses of curcumin in endoneurial fibroblast and Schwann cell cultures, evaluating their impact on cell viability and proliferation for prolonged periods of time.

Experimental desing for PDA polymerization/curcumin loading

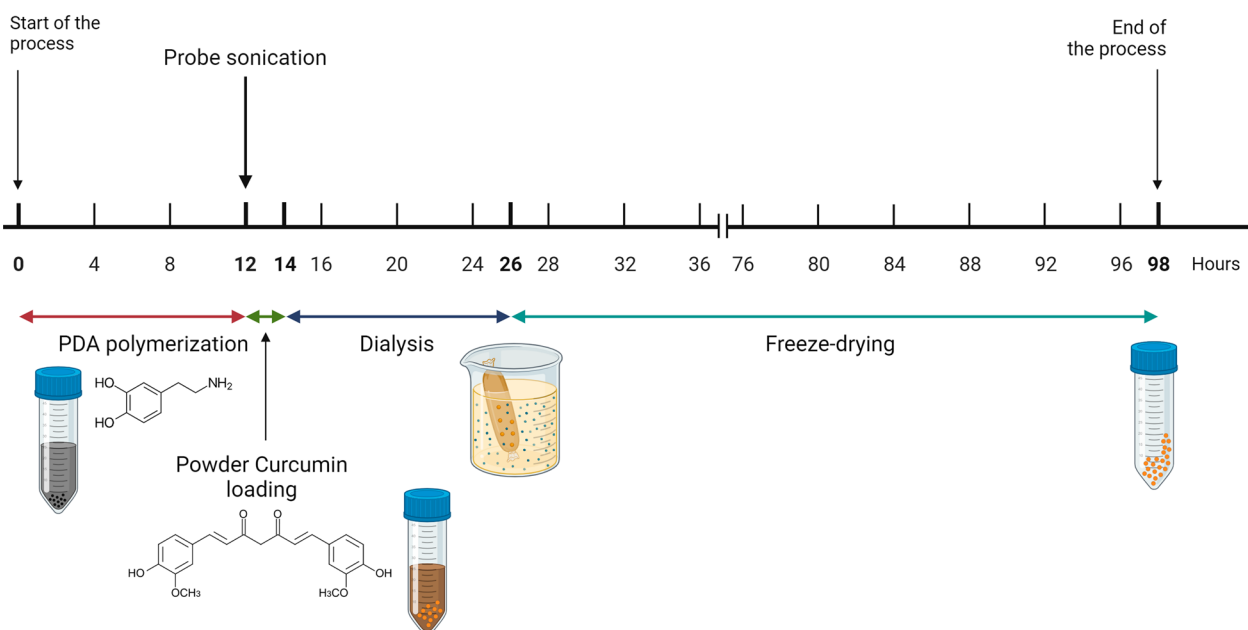


Fig. 1 Experimental design of PDA polymerization and curcumin loading. Polydopamine (PDA) nanoparticles were polymerized in TRIS–HCl buffer pH=8.5, 10 mM, for 12 h at RT, protected from light and under constant agitation. Then, a stem sonication was performed, followed by loading with curcumin powder (without organic solvents) for 2 h at RT, protected from light and under constant stirring. Dialysis was performed for 12 h at RT, protected from light and under constant stirring in a 14 kDa membrane. At the end of the time, the PDA or Curc-PDA was lyophilized for 72 h. The resulting powder is stored at 4 °C protected from light until use. The scheme was created with BioRender.com

2 Materials and methods

2.1 PDA fabrication and curcumin loading

Polydopamine nanoparticles (PDA) were polymerized with 10 mM dopamine hydrochloride (Cat#: H8502, Sigma-Aldrich, Taufkirchen, Germany) in TRIS–HCl (Cat#: 1185-53-1, Sigma-Aldrich, Taufkirchen, Germany) buffer pH = 8.5, 10 mM, for 12 h at room temperature (RT), protected from light and under constant agitation. Then, a probe sonication was performed, followed by loading with curcumin for 2 h at RT, protected from light and under constant stirring. For this, we incorporated the curcumin powder directly into the PDA solution so the curcumin is finally at a concentration of 10 mM. Dialysis was performed for 12 h at RT, protected from light and under stirring in a 14 kDa membrane (Cat#: D9527, Sigma-Aldrich, Taufkirchen, Germany). Finally, the PDA or Curcumin in PDA (Curc-PDA) was lyophilized for 72 h. The resulting powder was stored at 4 °C protected from light until use. The schematic model is shown in Fig. 1.

2.2 PDA and Curc-PDA transmission and scanning electron microscopy

The morphology and size of PDA and Curc-PDA in an aqueous solution were determined by transmission electron microscopy (TEM). For unloaded PDA, a suspension of 1.2 mg/ml (10 mM) was made in distilled water, which was then diluted 100-fold (100 μ M). For Curc-PDA, the same suspension was made, assuming a similar concentration, of the loaded nanoparticles. A sample drop (10 μ l) of PDA or Curc-PDA in distilled water was deposited on a 300-mesh

carbon-coated copper mesh, dried for 20 min at RT, and then, the sample was observed by TEM. The surface morphology of PDA and Curc-PDA were also observed by scanning electron microscopy (SEM). Using the same solutions as for TEM, 50 μ l was placed in blocks on a double-sided tape, dried at RT, and then metalized for SEB visualization.

2.3 Diffraction light scattering

The hydrodynamic diameter of the synthesized nanoparticles was determined using Dynamic Light Scattering (DLS) with a Nanoptic 90 instrument (BetterSize, China) operating at a wavelength (λ) of 635 nm and a scattering angle (θ) of 90°. The measurements were conducted at 25 °C, with the nanoparticles dispersed in a culture medium. Before analysis, the samples were sonicated in three cycles of 30 s each to ensure proper dispersion. The mean particle size was determined by averaging three measurements from a single sample.

2.4 HPLC experiments

2.4.1 UHPLC-MS analyses

LC-MS analyses were performed by an Ultimate 3000 UHPLC instrument coupled with an ISQ EC mass spectrometer, equipped with an electrospray ion source and a single-quadrupole analyzer (Thermo Fisher Scientific, Cambridge, MA, USA). A C18, Luna® Phenomenex, 5 μ m 100 Å (150 \times 4.6 mm) (Phenomenex, Torrance, CA, USA) was used for chromatographic separation. The mobile phase was composed of solvents A (Water, 0.1% HCOOH) and B (Acetonitrile, 0.1% HCOOH). An isocratic mode (30:70) was used. The flow rate was set at 0.2 mL/min and the column was maintained at 30 °C for the entire run. Fifty microliters were injected. Analyses were performed using the positive ionization mode selecting the following m/z: 91, 137, 154, 369. The collision energy (CE) was 20 eV. Mass spectrometry parameters were: spray voltage (V) 3000, sheath gas (arb) 28.8 psig, aux gas (arb) 3.2 psig, ion transfer tube temperature 300 °C, and vaporizer temp 117 °C. Peak areas were measured by using the Chromeleon software (Thermo Fisher Scientific).

2.4.2 Curcumin quantification in PDA

To determine the load of curcumin on PDA nanoparticles, 1 mg/ml solutions of Curcumin alone, unloaded PDA, and Curc-PDA in methanol were created. We then searched for curcumin by UHPLC-MS at m/z = 368 ion. We made three independent experiments, with duplicates of each sample. To calculate the curcumin concentration within the PDA; we used the area under the curve of the standard curcumin peak, of known concentration, and obtained the relationship to the area under the curve of the curcumin peak in the Curc-PDA sample.

2.4.3 Release-retention dynamics

To evaluate how curcumin was released from PDA to the culture medium, we studied its release dynamics during 24 h. To do so, we generated a 1 mg/ml solution of Curc-PDA in a culture medium and separated the solution into different tubes to have the samples at different times: 0.5, 1.0, 1.5, 2.0, and 24 h. At each time, the tube was centrifuged, and a sample of the supernatant was taken to look for curcumin released into the culture medium. Then, the medium was removed, replaced by an equal volume of methanol, and centrifuged one more time. As a result, we obtained the curcumin retained in the PDA, which was removed from the nanoparticle by methanol. Both samples were analyzed by UHPLC-MS at m/z = 368 ion, in three independent experiments.

2.5 Animals

C57BL wild-type (Wt) mice were obtained from Jackson Laboratories (JAX stock #002504, Jackson Laboratories, Bar Harbor, ME, USA). The colony was maintained at the Clemente Estable Biological Research Institute (IIBCE, MEC) bioterium. The local ethics committee approved all the experiments and procedures (Comisión de Ética en el Uso de

Animales (CEUA), IIBCE, Uruguay, protocol number: 002a/10/2020). The regulations and guidelines were followed according to Uruguayan Law number 18611 (<https://www.impo.com.uy/bases/leyes/18611-2009/8>). Mice were housed in a controlled environment (12 h light/dark cycle) and a mean temperature of 21 ± 3 °C with food and water-free access. This work used postnatal male mice 5 days old ($n = 5$ for each group).

2.6 Endoneurial fibroblasts and Schwann cell primary culture

Sciatic nerve fibers were dissected as previously described [30]. Briefly, after decapitation, both sciatic nerves were dissected using surgical scissors. The nerves were then immersed in Dulbecco's Modified Eagle's Medium (Cat#: DMEM-HSPTA, Capricorn, Ebsdorfergrund, Germany) supplemented with 10% Bovine Serum (FBS, Cat#: 26140079, Gibco™, Waltham, MA, USA); 5 µg/mL penicillin, 5 µg/mL streptomycin, 10 µg/mL neomycin (PSN 1X, Cat#: 15640055, Gibco™, Waltham, MA, USA). Immediately, the epineurium was removed and the fibers were teased under a stereoscopic microscope.

After, the fibers were incubated for 30 min at 37 °C to collagenase (WD: 225 µg/mL, Cat#: C9407, Sigma-Aldrich, Taufkirchen, Germany) in DMEM supplemented, and 5 mM CaCl₂. The fibers were centrifugated, the supernatant was removed and it was incubated for 30 min at 37 °C to trypsin (WD: 0.25%, Cat#: 15,090,046, Gibco™, Waltham, MA, USA) in DMEM with PSN 1X. Then, it was centrifugated and finally, the pellet was resuspended in DMEM supplemented, plated, and cultured at 37 °C and 5% CO₂. The next days, the culture was evaluated by an inverted light microscope for Schwann cells (SC) and endoneurial fibroblast (EFB) growth.

The medium was replaced every 48 h, and after one week to obtain SC and EFB enrichment cultures, we performed the cold jet procedure [55]. For SC culture, the medium was supplemented with 8 µM forskolin (Cat#: F6886, Sigma-Aldrich, Taufkirchen, Germany) and 20 µg/mL bovine pituitary extract (Cat#: P1167, Sigma-Aldrich, Taufkirchen, Germany). The last one was used in the experiments and was not further than passage 3.

2.7 Determination of the concentration of PDA suitable for cultures

To determine the concentration without affecting the cultures, viability, and proliferation assays were performed. The viability of the cultures was studied by 3-(4,5-Dimethylthiazol-2-yl)-2,5-Diphenyltetrazolium Bromide (MTT) assay and the proliferation was carried out with CyQUANT™ Cell Proliferation Assay (Cat#: C7026, Invitrogen, Eugene, OR, USA). For both assays, 1×10^5 cells per well were seeded, in a 96-well plate. 24 h later, the medium was removed and replaced by a medium containing different concentrations of PDA (0.32; 0.64; 1.93; 9.63; 19.25; 192.50; 1925 mg/l). The concentrations were evaluated in triplicate and three independent experiments were carried out. The treatment was conducted for five days, with medium changes every 24 h. We used untreated control as a control, being 100% of viability.

Every day, for viability the medium was removed and replaced by culture medium with the reagent MTT (Cat#: M6494, Invitrogen, Eugene, OR, USA), work dilution (WD): 0.5 mg/mL. This pale yellow, water-soluble compound is reduced in the presence of living cells, precipitating as formazan (violet-blue crystals, insoluble in water) [56]. The cells were incubated for 2 h at 37 °C and 5% CO₂. Then, the medium was removed and the cells were lysed with DMSO to release and solubilize the formazan crystals followed by absorbance measurements at 570 nm and 650 nm (background) in the Varioskan® (Varioskan® Flash, Thermo Fisher Scientific, Waltham, MA, USA). For proliferation, each day the medium was removed and replaced by 200 µl of the mixing kit per well, and after 5 min, we performed fluorescence measurements exiting at 480 nm and measuring the emission at 520 nm, in the Varioskan®.

2.8 Treatment with Curc-PDA

To study the effect of curcumin on culture viability and proliferation, a concentration of 0.05 µM curcumin in PDA was used, below the PDA concentration limit previously determined. Using the same approach as in the previous section, the analysis of MTT and CyQUANT was performed every 24 h, following the effect on the cultures for 5 days. We used PDA without curcumin as a control of 100% viability and made three independent experiments.

2.9 Statistical analysis

The normality of the data obtained was evaluated by the Shapiro–Wilk test. The analysis of released and retained compounds was performed with paired student t-test or Wilcoxon test, comparing the values obtained for each time

analyzed. Within each day, Viability and proliferation values for the different PDA concentrations were evaluated with one-way ANOVA, Bonferroni post hoc test, or Kruskal Wallis test, with Dunn's correction. Viability and proliferation values of cultures treated with PDA or with Curc-PDA were evaluated per day, with the unpaired Student's t-test or with the Mann–Whitney test. All tests were applied using a two-tailed distribution and the results were considered significant at an alpha level of 0.05. Statistical analysis was performed with GraphPad Prism version 8.0.0 (RRID: SCR_002798, GraphPad Software, San Diego, CA, USA).

3 Results

3.1 PDA structure and quantification of curcumin loading

The structure of unloaded and curcumin-loaded Polydopamine nanoparticles was determined by TEM and SEM (Fig. 2A and B). From the images obtained, the diameters of the nanoparticles were calculated. The unloaded PDA showed a diameter of 178 ± 5 nm, while the PDA loaded with curcumin had a diameter of 290 ± 7 nm. The frequency distribution shows the number of nanoparticles in each range, both PDA and Curc-PDA, with a clear area of overlap between these structures (Fig. 2C). DLS analysis showed that PDA nanoparticles exhibited sizes ranging from 100 to 185 nm, with an average diameter of 144 nm. In contrast, the Curc-PDA displayed larger sizes, ranging from 150 to 300 nm, with an average diameter of 223 nm (Fig. 2D). Both samples showed polydispersity, evidenced by values between 0.26 and 0.37 respectively.

To determine the amount of curcumin in the PDA, we measured curcumin by UHPLC-MS, releasing it from the PDA with the addition of methanol (Fig. 2E). This compound was evaluated at 369 mass–charge-ion ($m/z = 369$) and showed a peak at a retention time of 17.5 ± 0.5 min. Compared with the standard of Curcumin in methanol at the same concentration, we found the concentration of curcumin in the PDA was 0.65 ± 0.04 mg/ml (Fig. 2, table), from the curcumin standard and the unloaded PDA control (Additional file 1: Table S1). Given that the concentration of loaded and unloaded PDA was 1 mg/ml, the results show that for each milligram of loaded nanoparticle, we have 0.65 mg of curcumin, i.e., 65% corresponds to curcumin, while 35% corresponds to PDA.

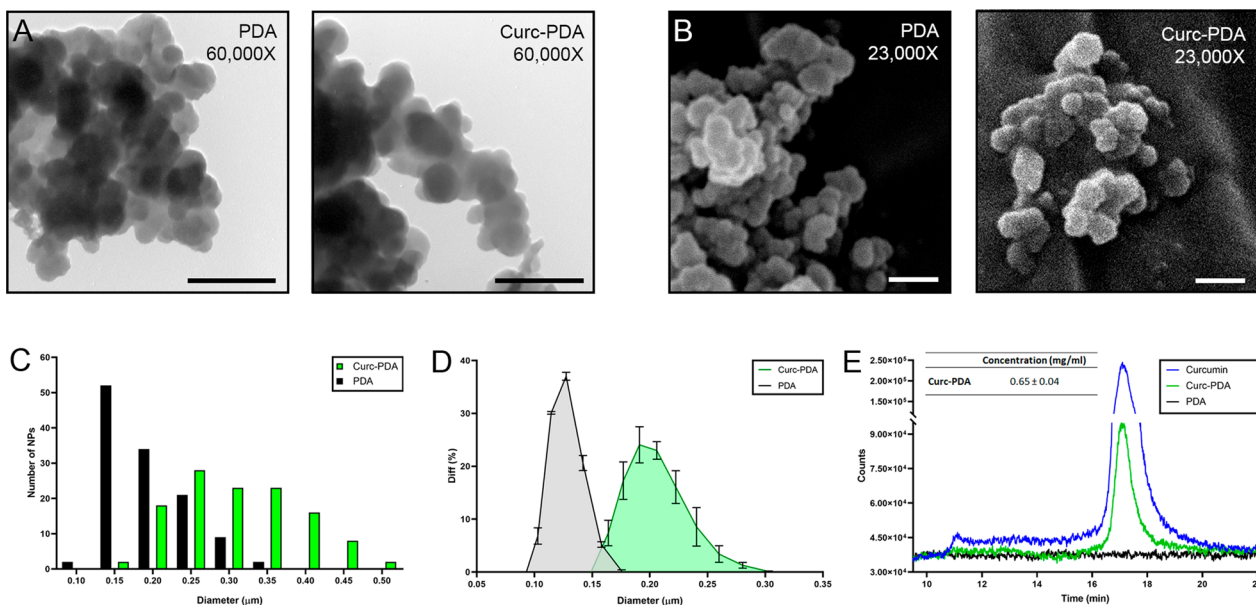


Fig. 2 PDA structure and quantification of curcumin loading. **A** Transmission electron microscopy images of 100 μM unloaded (PDA) and curcumin-loaded (Curc-PDA) Nanoparticles. **B** Scanning electron microscopy images of 100 μM PDA and Curc-PDA. **C** Frequency diagram of the diameters obtained by electron microscopy. **D** PDA and Curc-PDA diameters obtained by diffraction light scattering analysis. **E** Spectra obtained by UHPLC-MS of samples solubilized in methanol at 1 mg/ml of curcumin, PDA, or Curc-PDA. By area integration, it is obtained that the concentration of curcumin loaded in the nanoparticles is expressed as mean ± SEM. Scale: 0.5 μm

3.2 Release dynamics of Curc-PDA in the culture medium

The release dynamics of curcumin were evaluated at different times: 0.5, 1.0, 1.5, 2.0, and 24 h, assessing at each time, the presence of curcumin in the culture medium by UHPLC-MS (Fig. 3).

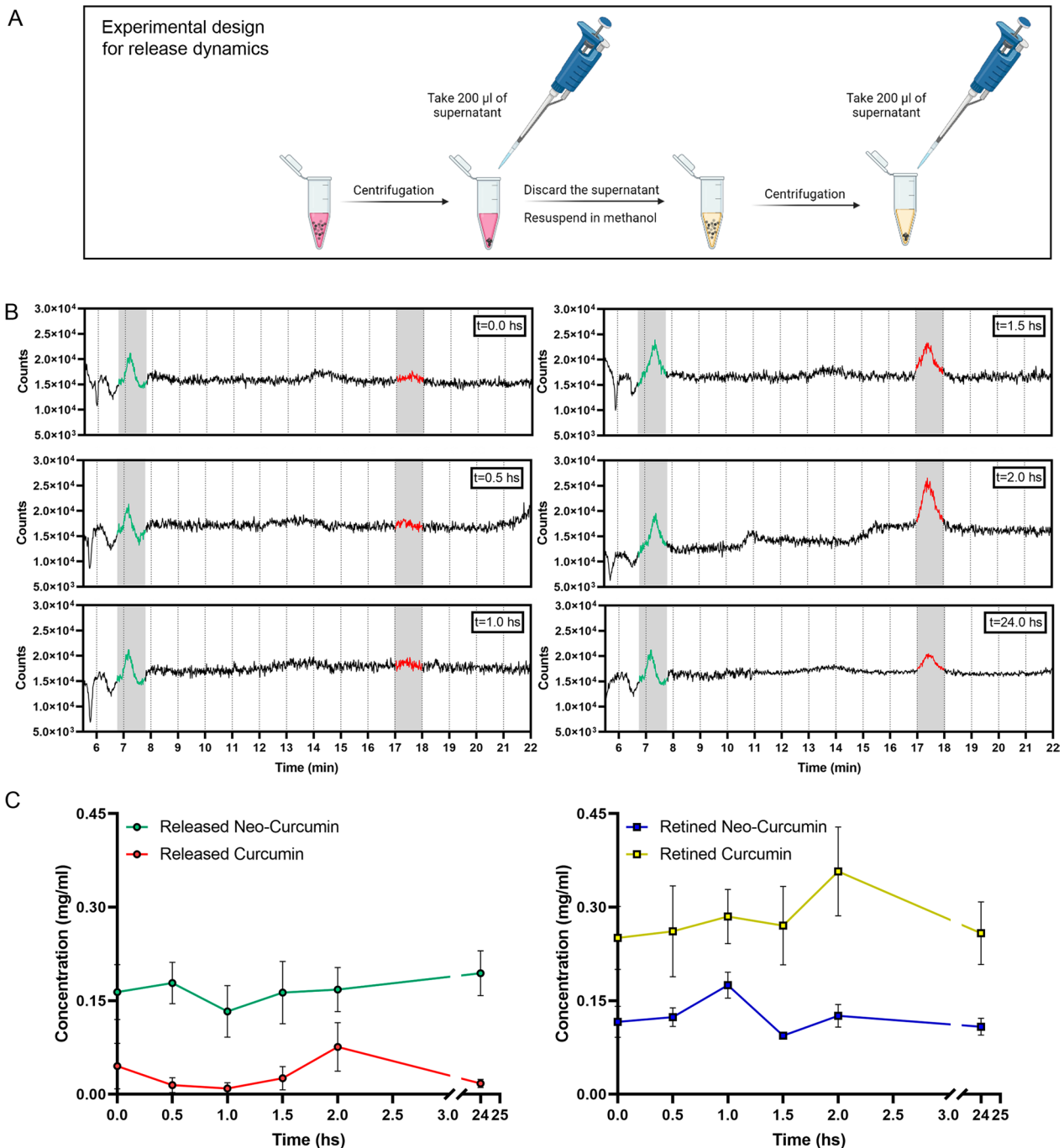


Fig. 3 Release dynamics of Curc-PDA in the culture medium. Curcumin-loaded nanoparticles were placed in a culture medium, and the presence of curcumin released to the medium and retained in PDA was evaluated after 0.5, 1.0, 1.5, 2.0, and 24 h. **A** Experimental design created with BioRender.com. **B** Spectra obtained by UHPLC-MS, $m/z=369$, for the released curcumin. Red indicates the characteristic peak of curcumin. Green means the presence of a species with the same m/z , detected at all times and in the ferulic acid standard (the latter in Additional file 1: Figure S4), which we call Neo-Curcumin. **C** Variation of the released and retained concentration and neo-curcumin concentration over time. Each point indicates the mean \pm SEM

For all times, the release diagrams show the presence of the characteristic peak of curcumin (Fig. 3A in red) at the reported retention time, but also show the presence of a new compound, with the same m/z ratio, but with a shorter retention time, 7.3 ± 0.5 min (Fig. 3A in green), which we will call neo-curcumin. Additionally, the concentrations of curcumin retained in the PDA at different times were measured by UHPLC-MS (Additional file 1: Fig. S1). The concentrations obtained from the areas under the curve are visualized in Fig. 3C. The released curcumin shows a peak of maximum concentration at 2 h and after 24 h in the medium, it is almost imperceptible. In contrast, neo-curcumin shows a concentration without variations over time, with an average of 17.5 ± 0.4 mg/ml (Fig. 3B left). In the case of retained curcumin, we found that both curcumin and neo-curcumin presented higher concentrations after 24 h (Fig. 3B right).

3.3 Determination of the PDA concentration without-biological detectable effect in cell cultures

To determine the maximum non-toxic PDA concentration for the cultures, we evaluated two cellular parameters: viability and proliferation (Fig. 4). The cultures were treated with different concentrations of unloaded PDA, ranging from 0.32 mg/l to 1925 mg/l. Based on the previous result of curcumin loading on PDA, these unloaded PDA concentrations allow loading from 0.1 μ M to 600 μ M curcumin. For each concentration tested, 5 replicates of the culture were generated, to analyze the changes of these cell parameters daily. Those wells that did not receive treatment on that day had their medium changed to the corresponding PDA concentration. The viability was measured with an MTT assay (Fig. 4A). Of the concentrations tested, only 0.32 mg/l was the concentration that showed no difference compared to the control, during the five days of treatment. The rest of the concentrations showed differences on the fifth day of treatment. The proliferation was measured with the CyQUANT assay (Fig. 4B). With this assay, we found three concentrations that did not differ from the control, 0.32, 0.64, and 1.93 mg/ml. Since 0.32 was the only concentration that coincided in both parameters, with no toxic effects on the cultures, we decided to continue our evaluation using this concentration of PDA.

3.4 Effects on viability and proliferation of endoneurial fibroblast cultures treated with Curc-PDA.

Once the working concentration of PDA was defined as non-toxic to our cultures, we evaluated the effect of curcumin treatment in PDA on the viability and proliferation of the cultures. To be below the established PDA limit, we decided to evaluate the effects of 0.05 μ M curcumin (Fig. 5).

In the case of viability, from the second day of treatment, we observed an increase in the number of cells when cultures were treated with Curc-PDA ($p=0.002$), which was maintained on the following days of treatment (day 3: $p=0.002$; day 4: $p=0.001$; day 5: $p=0.04$) (Fig. 5A). If we also evaluated the percentage of accumulated growth, taking as a reference the beginning of the treatment, we find that from the second day onwards all the percentages obtained in cultures treated with Curc-PDA show significant differences with both the control without treatment and the control with unloaded PDA ($p < 0.0001$) (Fig. 5C). Comparison of the values obtained with Curc-PDA indicates a significant increase between the first and second day of treatment ($p=0.03$), while between the second, third, fourth, and fifth day, there is no significant difference (Additional file 1: Fig. S2A).

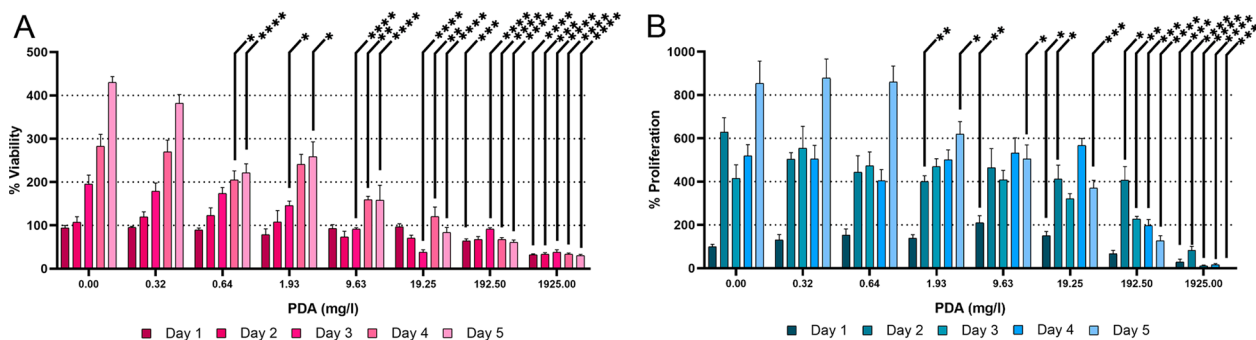


Fig. 4 Determination of the no-effect PDA concentration in cell cultures. Before PDA loading, the maximum no-effect PDA concentration on endoneurial fibroblast cultures was determined. During the 5-day treatment, the cultures were tested every day for **A** Viability (by MTT assay) and **B** Proliferation (by CyQUANT assay). The graphs show the percentage of the untreated control on day 0 (before the experiment started). Median \pm SIR is plotted

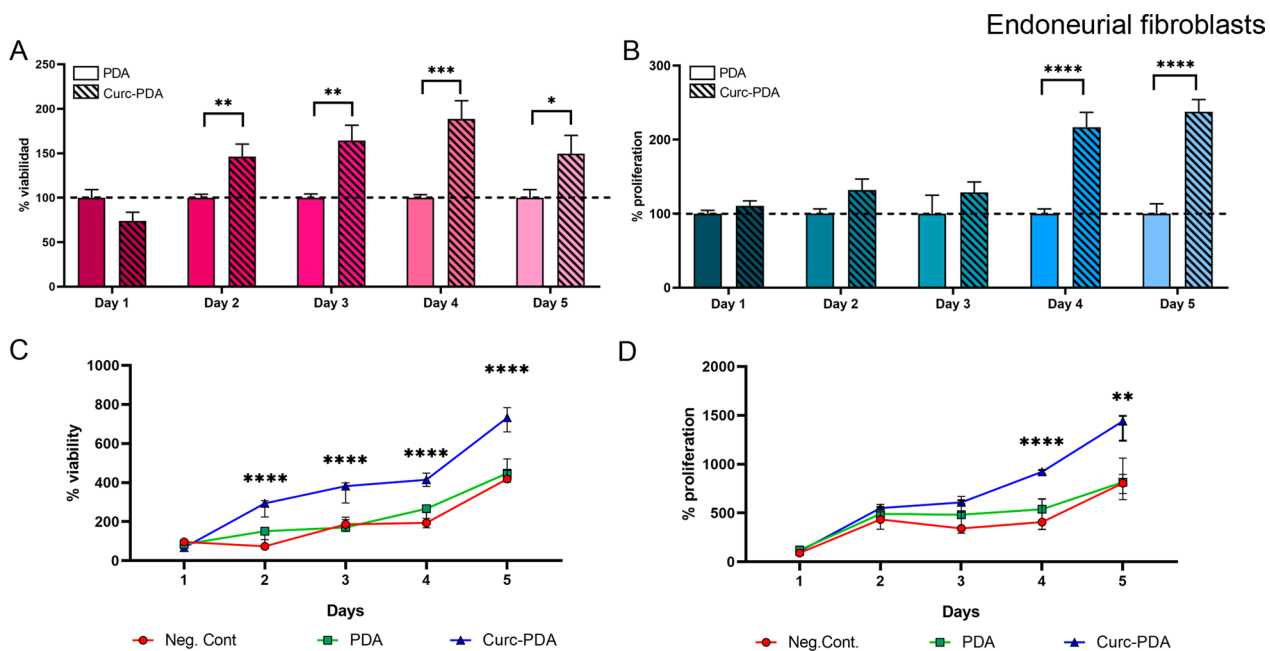


Fig. 5 Effects on viability and proliferation of endoneurial fibroblast cultures treated with Curc-PDA. Cultures of endoneurial fibroblasts were treated with PDA (0.32 mg/l) and Curc-PDA (0.05 μ M curcumin) for 5 days, assessing daily: **A** Viability (by MTT assay) and **B** Proliferation (by CyQUANT assay). The graphs show the percentage of PDA-treated cultures on the same day. **C** Cumulative viability. **D** Cumulative proliferation. Values reported for the first day of treatment. **D**. Median \pm SIR is plotted

The values obtained for proliferation showed an increase in the values with Curc-PDA during the fourth and fifth day of treatment, to the control with unloaded PDA ($p < 0.0001$) (Fig. 5B). In this sense, the evaluation of cumulative proliferation during the 5 days of treatment also shows an increase in the Curc-PDA treated cultures compared to the negative control and the unloaded PDA control on both the fourth and fifth day (day 4: $p < 0.0001$; day 5: $p = 0.004$) (Fig. 5D). These results also concur with the comparison of percentages during the whole treatment with Curc-PDA, where an increase of this parameter is visualized between the third and fourth day ($p = 0.0002$), a difference that is maintained until the fifth day (Additional file 1: Fig. S2B).

3.5 Effects on viability and proliferation of Schwann cell cultures treated with Curc-PDA

The effects of viability and proliferation on Schwann cell culture after treatment with Curc-PDA were evaluated, using the same curcumin concentration that endoneurial fibroblast (Fig. 6).

Both viability and proliferation showed the same pattern for SCs as for EFBs: compared to Curc-PDA vs PDA treatments, viability increased and then remained constant after two-day (day 2: $p = 0.002$; day 3: $p = 0.006$; day 4: $p = 0.03$; day 5: $p = 0.009$) (Fig. 6A); whereas proliferation increased after four-day treatment and maintained that difference in the last day of treatment ($p < 0.0001$) (Fig. 6B).

About the percentage of accumulated growth, we find that viability from the second day onwards all the percentages obtained in cultures treated with Curc-PDA show significant differences with both the control without treatment and the control with unloaded PDA (day 3: $p = 0.002$; day 4: $p < 0.0001$; day 5: $p = 0.0025$) (Fig. 6C).

4 Discussion

In the present work, we have characterized polydopamine nanoparticles (PDA), determining their structure and their curcumin-loaded profile (Curc-PDA). In this process, we completely eliminated the use of any organic solvent to dissolve curcumin, which we consider makes a huge difference in our biological model of SCs and EFBs cell culture. In fact, we have already reported the sensitivity of SCs to the toxic action of ethanol and DMSO as a vehicle for curcumin [30].

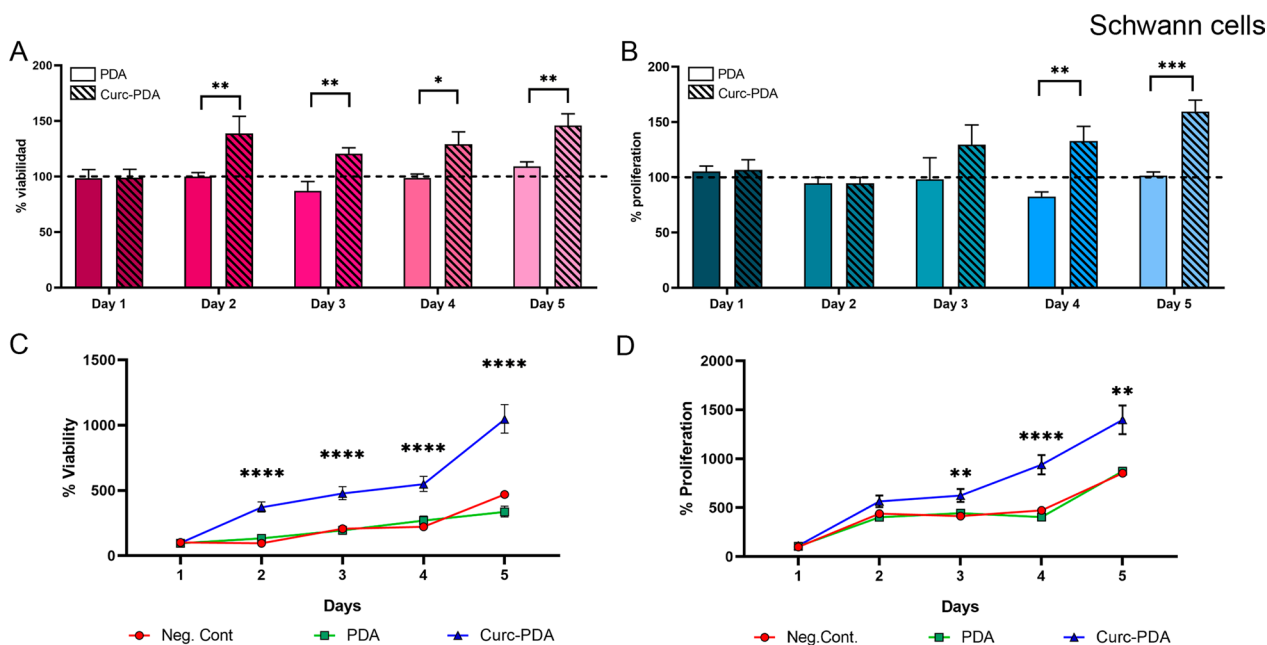


Fig. 6 Effects on viability and proliferation of endoneurial fibroblast cultures treated with Curc-PDA. Cultures of endoneurial fibroblasts were treated with PDA (0.32 mg/l) and Curc-PDA (0.05 μ M curcumin) for 5 days, assessing daily: **A** Viability (by MTT assay) and **B**. Proliferation (by CyQUANT assay). The graphs show the percentage of PDA-treated cultures on the same day. **C** Cumulative viability. **D** Cumulative proliferation. Values reported for the first day of treatment D. Median \pm SIR is plotted

In general, the use of curcumin is always accompanied by a solubilization stage, whatever the vehicle strategy [21, 27, 28, 52] and this introduces an extra variable in the analysis of the results obtained. This is why building nanoparticles with curcumin, without the use of organic solvents, and knowing the maximum concentration of PDA use without toxic effect on crops (0.32 mg/l), allows us to evaluate the effects and attribute them completely to the use of curcumin (0.05 μ M), loaded in that harmless concentration of PDA. The approach shown in this work represents a novelty in the procedure of its delivery, where one of its main virtues is based on the elimination of the undesirable effect of the carrier used. Additionally, taking into account the pH dependence that curcumin release has shown in different contexts [49–52], we understand that the incorporation of the dialysis step after the curcumin-loaded nanoparticles has resulted in a significant improvement in the quality of the nanoparticles obtained and in their innocuousness as a carrier at the biological level.

The unloaded PDA nanoparticles were found to be smaller in size than the curcumin-loaded nanoparticles, as determined by TEM, SEM, and DLS. TEM measurements corroborated the trend observed in the DLS results (Fig. 2C and D). However, it should be noted that the particle sizes determined by TEM are larger than those determined by DLS. The DLS technique assesses the size of nanoparticles in the hydrated state, which results in a hydrodynamic diameter typically larger than the particle diameter determined by TEM [57]. The difference in our results can be attributed to the agglomeration of nanoparticles during sample preparation for TEM analysis. Incorporating a sonication step before mounting the nanoparticles on the grids could be an alternative to obtain a higher dispersion of the nanoparticles. Nevertheless, TEM and DLS showed equivalent values in their measurements.

After characterization, we evaluated the release of curcumin from PDA in a culture medium, at different times for 24 h. This allows us to identify that curcumin, detected by UHPLC-MS at a retention time of 17.5 min in the ion $m/z=369$, has a peak of maximum released at 2 hs, but then its concentration decays, being very low at 24 hs. In parallel, the concentration of curcumin retained in the PDA was also analyzed by UHPLC-MS (Additional file 1: Fig. S1 in yellow). At all analyzed times, the retained curcumin concentration was higher than the released curcumin, from PDA nanoparticles. Also, we detected another peak, at a retention time of 7.3 min. This peak was detected in both the release (Fig. 3B in green) and retention analyses (Additional file 1: Fig. S1 in blue), with concentrations in both cases in the region of 0.15 mg/ml (Fig. 3C in green and blue). This compound has the same mass charge as curcumin, $m/z=369$, with the retention time on the column being different. This peak, which we call neo-curcumin, is not present in the chromatographic profile control only with medium culture, nor with unloaded PDA (1 mg/ml) (Additional file 1: Fig. S3). Since neo-curcumin has the same mass, it is possibly a rearrangement or conformational change of the molecule, without chemical changes, such as a curcumin

rotamer or tautomer. Chatterjee et al., 2022, recently reported the existence of rotamers in curcumin [58]. Based on that, we can hypothesize that in our loading conditions, the neo-curcumin released at 7.3 min corresponds to a rotamer of lower hydrophobicity than the “cannonic” curcumin, released at 17.5 min. To understand where this neo-curcumin peak was coming from, we decided to evaluate the standard of the major degradation product of curcumin, ferulic acid [59, 60]. To do so, we studied its ion $m/z = 195$ and the corresponding ion-curcumin (Additional file 1: Fig. S4). The obtained results for the standard ferulic acid (1 mg/ml in methanol) indicate the presence of a peak at the m/z 369 ion, similar to that found in neo-curcumin.

Neo-curcumin and curcumin represent the highest percentage of compounds obtained from curcumin initially loaded on PDA nanoparticles ($88.17 \pm 1.74\%$). However, between the two, neo-curcumin represents the largest component released (about 85% of the total released), in a sustained manner over time. Concerning the biological impact of curcumin delivered, we hypothesize that the effects on viability and proliferation observed in SCs and EFBs may be mainly due to these forms of curcumin released from the Curc-PDA nanoparticles. We do not rule out the possibility of characterizing the presence of other curcumin derivatives, which, given their low concentration, represent a challenge.

Exposure of cell culture to $0.05 \mu\text{M}$ curcumin in PDA for 5 days allowed us to observe changes in viability and proliferation (Fig. 5). These changes appeared with a lag time but, when they increased, they were maintained over time: while the increase in viability occurred on the second day of treatment, proliferation increased on the fourth day of treatment for SCs and EFBs (Additional file 1: Fig. S2). However, both parameters did not increase after the initial ones and remained constant until the end of treatment. This result shows that proliferation and also viability respond to the impact of curcumin action in a limited and stable manner, in long-term treatments.

As the viability assay used is the MTT, the results allow us to consider a scenario in which curcumin initially has an impact on the metabolic activity level, including mitochondrial activity or its modulation, increasing the viability. Subsequently, perhaps the direct action of curcumin and/or the accumulative effect of the metabolic and mitochondrial implications, changes in proliferation are observed at the end of the treatment in both cellular types. Moreover, in SCs, we have already reported an increase in ribosomes due to the action of curcumin [30]. In this regard, mTOR is one of the proteins that could connect mitochondrial activity with protein synthesis processes, on which biosynthesis and cell proliferation depend [61]. For this reason, our future work aims to determine the expression of this multiprotein complex to reveal through which mechanisms these processes are connected.

Regarding the dose–response phenomena, called hormesis, our results can be classified within the beneficial effects observable at low concentrations of the compound, in this case, curcumin, applied for prolonged periods. This is because there are reports of the use of working concentrations, similar to ours, related to different beneficial effects in cultures: decreases in reactive oxygen species (ROS) [33], increase in members of the chaperone response pathways, autophagy and mTOR [12, 30], and cell regeneration increase [38, 62]. In contrast, doses in cultures from $40 \mu\text{M}$ onwards show clear lethal effects, applying curcumin as a potent antitumor [8, 20].

5 Conclusion

Given this broad spectrum of curcumin’s action, our main contribution lies in the characterization of a harmless curcumin’s vehicle, which guarantees not only that the observed effects can be related to the curcumin and their derivatives supply, but also that they allow a sustained and predictable release over time. Also, our findings contribute to the characterization of nanoparticles as a tool of particular value for in vitro studies focused on the dose/effect relationship over prolonged periods, for drug research and therapeutic purposes. In our current approach, it has allowed us to accurately assess the hormetic effect of curcumin.

Acknowledgements We would like to give special thanks to Dr. Gabriela Casanova, head of the Electron Microscopy Unit of the Facultad de Ciencias de la Universidad de la República, and her collaborators MSc. Magela Rodao and Dr. Gaby Martínez, for their kind collaboration in the visualization of the nanoparticles by TEM and SEM. We would also like to give special thanks to Dr. Susana Castro, head of the Sección Bioquímica of the Facultad de Ciencias de la Universidad de la República, and her collaborator MSc. Celica Cagide, for their kind collaboration in nanoparticle lyophilization.

Author contributions Conceptualization, L.V.A., M.C., and A.K.; methodology, L.V.A., and A.K.; software, L.V.A., M.M.B., E.A., C.E., and A.K.; validation, L.V.A., M.C., and A.K.; formal analysis, L.V.A., and A.K.; investigation, L.V.A., M.M.B., E.A., C.E., and A.K.; resources, A.K.; data curation, L.V.A., and A.K.; writing-original draft preparation, L.V.A., and A.K.; writing-review and editing, L.V.A., M.M.B., E.A., C.E., M.C., and A.K.; visualization, L.V.A. and A.K.; supervision, A.K.; project administration, A.K.; funding acquisition, M.C., A.K. All authors have read and agreed to the published version of the manuscript.

Funding This work was supported by Agencia Nacional de Investigación e Innovación (ANII), Uruguay [grant numbers: FCE_1_2019_1_155539; POS_NAC_2022_1_173578], the PEDECIBA, CSIC-UdelaR and SNI-ANII. From the Spanish, Ministry of Science and Innovation and the Spanish CIBERNED network [grant PID2019-110401RB-100].

Data availability Data available on request due to restrictions e.g., privacy or ethical. The data presented in this study are available on request from the corresponding author.

Declarations

Competing interests The authors declare no competing interests.

Open Access This article is licensed under a Creative Commons Attribution 4.0 International License, which permits use, sharing, adaptation, distribution and reproduction in any medium or format, as long as you give appropriate credit to the original author(s) and the source, provide a link to the Creative Commons licence, and indicate if changes were made. The images or other third party material in this article are included in the article's Creative Commons licence, unless indicated otherwise in a credit line to the material. If material is not included in the article's Creative Commons licence and your intended use is not permitted by statutory regulation or exceeds the permitted use, you will need to obtain permission directly from the copyright holder. To view a copy of this licence, visit <http://creativecommons.org/licenses/by/4.0/>.

References

1. Tomren MA, Másson M, Loftsson T, Tønnesen HH. Studies on curcumin and curcuminoids. XXXI. Symmetric and asymmetric curcuminoids: stability, activity and complexation with cyclodextrin. *Int J Pharm.* 2007;338:27–34. <https://doi.org/10.1016/j.ijpharm.2007.01.013>.
2. González-Albadalejo J, Sanz D, Lavandera JL, et al. Curcumin and curcuminoids: chemistry, structural studies and biological properties. *An Real Acad Nac Farm.* 2015;33:278–310.
3. Shakeri A, Cícero AFG, Panahi Y, et al. Curcumin: a naturally occurring autophagy modulator. *J Cell Physiol.* 2019;234:5643–54. <https://doi.org/10.1002/jcp.27404>.
4. Lestari MLAD, Indrayanto G (2014) Curcumin. In: Profiles of drug substances, excipients and related methodology. Academic Press Inc., pp 113–204
5. Wong TF, Takeda T, Li B, et al. Curcumin targets the AKT-mTOR pathway for uterine leiomyosarcoma tumor growth suppression. *Int J Clin Oncol.* 2014;19:354–63. <https://doi.org/10.1007/s10147-013-0563-4>.
6. Mao JL, Xiong X, Gong H. Effects of curcumin on tumor growth and immune function in prostate cancer-bearing mice. *Natl J Androl.* 2019;25:590–4.
7. Zhang W, Li Q, Yang C, et al. Curcumin exerts anti-tumor effects on diffuse large B cell lymphoma via regulating PPAR γ expression. *Biochem Biophys Res Commun.* 2020;524:70–6. <https://doi.org/10.1016/j.bbrc.2019.12.129>.
8. Beevers CS, Li F, Liu L, Huang S. Curcumin inhibits the mammalian target of rapamycin-mediated signaling pathways in cancer cells. *Int J Cancer.* 2006;119:757–64. <https://doi.org/10.1002/ijc.21932>.
9. Wright JS. Predicting the antioxidant activity of curcumin and curcuminoids. *J Mol Struct.* 2002;591:207–17. [https://doi.org/10.1016/S0166-1280\(02\)00242-7](https://doi.org/10.1016/S0166-1280(02)00242-7).
10. Motaghinejad M, Motevalian M, Fatima S, et al. Curcumin confers neuroprotection against alcohol-induced hippocampal neurodegeneration via CREB-BDNF pathway in rats. *Biomed Pharmacother.* 2017;87:721–40. <https://doi.org/10.1016/j.biopha.2016.12.020>.
11. Perrone L, Squillaro T, Napolitano F, et al. The autophagy signaling pathway: a potential multifunctional therapeutic target of curcumin in neurological and neuromuscular diseases. *Nutrients.* 2019. <https://doi.org/10.3390/nu11081881>.
12. Kang SK, Cha SH, Jeon HG. Curcumin-induced histone hypoacetylation enhances caspase-3-dependent glioma cell death and neurogenesis of neural progenitor cells. *Stem Cells Dev.* 2006;15:165–74. <https://doi.org/10.1089/scd.2006.15.165>.
13. Peng Y, Ao M, Dong B, et al. Anti-inflammatory effects of curcumin in the inflammatory diseases: status, limitations and countermeasures. *Drug Des Dev Ther.* 2021;15:4503–25. <https://doi.org/10.2147/DDDT.S327378>.
14. Kohli K, Ali J, Ansari MJ, Raheman Z. Curcumin: a natural antiinflammatory agent. *Indian J Pharmacol.* 2005;37:141. <https://doi.org/10.4103/0253-7613.16209>.
15. Barzegar A, Moosavi-Movahedi AA. Intracellular ROS protection efficiency and free radical-scavenging activity of curcumin. *PLoS ONE.* 2011;6:1–7. <https://doi.org/10.1371/journal.pone.0026012>.
16. Caillaud M, Chantemargue B, Richard L, et al. Local low dose curcumin treatment improves functional recovery and remyelination in a rat model of sciatic nerve crush through inhibition of oxidative stress. *Neuropharmacology.* 2018;139:98–116. <https://doi.org/10.1016/j.neuropharm.2018.07.001>.
17. Shinojima N, Yokoyama T, Kondo Y, Kondo S. Roles of the Akt/mTOR/p70S6K and ERK1/2 signaling pathways in curcumin-induced autophagy. *Autophagy.* 2007;3:635–7. <https://doi.org/10.4161/auto.4916>.

18. Forouzanfar F, Read MI, Barreto GE, Sahebkar A. Neuroprotective effects of curcumin through autophagy modulation. *IUBMB Life*. 2020;72:652–64. <https://doi.org/10.1002/iub.2209>.
19. Maiti P, Manna J, Veleri S, Frautschy S. Molecular chaperone dysfunction in neurodegenerative diseases and effects of curcumin. *Biomed Res Int*. 2014. <https://doi.org/10.1155/2014/495091>.
20. Odot J, Albert P, Carlier A, et al. In vitro and in vivo anti-tumoral effect of curcumin against melanoma cells. *Int J Cancer*. 2004;111:381–7. <https://doi.org/10.1002/ijc.20160>.
21. Abuelba H, Cotrutz CE, Stoica BA, et al. In vitro evaluation of curcumin effects on breast adenocarcinoma 2D and 3D cell cultures. *Rom J Morphol Embryol*. 2015;56:71–6.
22. Turturro A, Hass BS, Hart RW. Does caloric restriction induce hormesis? *Hum Exp Toxicol*. 2000;19:320–9. <https://doi.org/10.1191/096032700678815981>.
23. Masoro EJ. Role of hormesis in life extension by caloric restriction. *Dose-Response*. 2007;5:163–73. <https://doi.org/10.2203/dose-response.06-005.masoro>.
24. Calabrese EJ, Baldwin LA. Hormesis: the dose-response revolution. *Ann Rev Pharmacol Toxicol*. 2003;43(1):175–97. <https://doi.org/10.1146/annurev.pharmtox.43.100901140223>.
25. Soh JW, Marowsky N, Nichols TJ, et al. Curcumin is an early-acting stage-specific inducer of extended functional longevity in *Drosophila*. *Exp Gerontol*. 2013;48:229–39. <https://doi.org/10.1016/j.exger.2012.09.007>.
26. Watson JL, Hill R, Yaffe PB, et al. Curcumin causes superoxide anion production and p53-independent apoptosis in human colon cancer cells. *Cancer Lett*. 2010;297:1–8. <https://doi.org/10.1016/j.canlet.2010.04.018>.
27. Tello Velasquez J, Watts ME, Todorovic M, et al. Low-dose curcumin stimulates proliferation, migration and phagocytic activity of olfactory ensheathing cells. *PLoS ONE*. 2014;9:1–15. <https://doi.org/10.1371/journal.pone.0111787>.
28. Zhao Z, Li X, Li Q. Curcumin accelerates the repair of sciatic nerve injury in rats through reducing Schwann cells apoptosis and promoting myelination. *Biomed Pharmacother*. 2017;92:1103–10. <https://doi.org/10.1016/j.biopha.2017.05.099>.
29. Galvao J, Davis B, Tilley M, et al. Unexpected low-dose toxicity of the universal solvent DMSO. *FASEB J*. 2014;28:1317–30. <https://doi.org/10.1096/fj.13-235440>.
30. Vázquez Alberdi L, Rosso G, Velóz L, et al. Curcumin and ethanol effects in trembler-J Schwann cell culture. *Biomolecules*. 2022;12:1–19. <https://doi.org/10.3390/biom12040515>.
31. Adler S, Pellizzer C, Paparella M, et al. The effects of solvents on embryonic stem cell differentiation. *Toxicol In Vitro*. 2006;20:265–71. <https://doi.org/10.1016/j.tiv.2005.06.043>.
32. Ilieva Y, Dimitrova L, Zaharieva MM, et al. Cytotoxicity and microbicidal activity of commonly used organic solvents: a comparative study and application to a standardized extract from *Vaccinium macrocarpon*. *Toxics*. 2021;9:92. <https://doi.org/10.3390/toxics9050092>.
33. Caillaud M, Msheik Z, Ndong-Ntoutoume GMA, et al. Curcumin–cyclodextrin/cellulose nanocrystals improve the phenotype of Charcot-Marie-Tooth-1A transgenic rats through the reduction of oxidative stress. *Free Radic Biol Med*. 2020;161:246–62. <https://doi.org/10.1016/j.freeradbiomed.2020.09.019>.
34. Ndong Ntoutoume GMA, Granet R, Mbakidi JP, et al. Development of curcumin-cyclodextrin/cellulose nanocrystals complexes: new anticancer drug delivery systems. *Bioorg Med Chem Lett*. 2016;26:941–5. <https://doi.org/10.1016/j.bmcl.2015.12.060>.
35. Kim CY, Bordenave N, Ferruzzi MG, et al. Modification of curcumin with polyethylene glycol enhances the delivery of curcumin in preadipocytes and its antiadipogenic property. *J Agric Food Chem*. 2011;59:1012–9. <https://doi.org/10.1021/jf103873k>.
36. Haukvik T, Bruzell E, Kristensen SD, Tønnesen HH. Photokilling of bacteria by curcumin in selected polyethylene glycol 400 (PEG 400) preparations: studies on curcumin and curcuminoids, XLI. *Pharmazie*. 2010;65:600–6. <https://doi.org/10.1691/ph.2010.0048>.
37. de Carvalho DM, Takeuchi KP, Geraldine RM, et al. Production, solubility and antioxidant activity of curcumin nanosuspension. *Food Sci Technol (Brazil)*. 2015;35:115–9. <https://doi.org/10.1590/1678-457X.6515>.
38. Liu X, You L, Tarafder S, et al. Curcumin-releasing chitosan/alginate membrane for skin regeneration. *Chem Eng J*. 2019;359:1111–9. <https://doi.org/10.1016/j.cej.2018.11.073>.
39. Requejo-Aguilar R, Alastrue-Agudo A, Cases-Villar M, et al. Combined polymer-curcumin conjugate and ependymal progenitor/stem cell treatment enhances spinal cord injury functional recovery. *Biomaterials*. 2017;113:18–30. <https://doi.org/10.1016/j.biomaterials.2016.10.032>.
40. Stohs SJ, Chen O, Ray SD, et al. Highly bioavailable forms of curcumin and promising avenues for curcumin-based research and application: a review. *Molecules*. 2020;25:1–12. <https://doi.org/10.3390/molecules25061397>.
41. Chen Y, Lu Y, Lee RJ, Xiang G. Nano encapsulated curcumin: and its potential for biomedical applications. *Int J Nanomed*. 2020;15:3099–120. <https://doi.org/10.2147/IJN.S210320>.
42. Sohn SI, Priya A, Balasubramaniam B, et al. Biomedical applications and bioavailability of curcumin—an updated overview. *Pharmaceutics*. 2021. <https://doi.org/10.3390/pharmaceutics13122102>.
43. McNamara K, Tofail SAM. Nanoparticles in biomedical applications. *Adv Phys X*. 2017;2:54–88.
44. Bilal M, Zhao Y, Rasheed T, Iqbal HMN. Magnetic nanoparticles as versatile carriers for enzymes immobilization: a review. *Int J Biol Macromol*. 2018;120:2530–44.
45. Mokhtarzadeh A, Alibakhshi A, Yaghoobi H, et al. Recent advances on biocompatible and biodegradable nanoparticles as gene carriers. *Expert Opin Biol Ther*. 2016;16:771–85.
46. Alfieri ML, Weil T, Ng DYW, Ball V. Polydopamine at biological interfaces. *Adv Colloid Interface Sci*. 2022;305:1–14.
47. Li J, Chen L, Zhang X, Guan S. Enhancing biocompatibility and corrosion resistance of biodegradable Mg-Zn-Y-Nd alloy by preparing PDA/HA coating for potential application of cardiovascular biomaterials. *Mater Sci Eng C*. 2020;109:110607. <https://doi.org/10.1016/j.msec.2019.110607>.
48. Liebscher J. Chemistry of polydopamine—scope, variation, and limitation. *Eur J Org Chem*. 2019;2019:4976–94. <https://doi.org/10.1002/ejoc.201900445>.
49. Pan H, Shen X, Tao W, et al. Fabrication of polydopamine-based curcumin nanoparticles for chemical stability and pH-responsive delivery. *J Agric Food Chem*. 2020;68:2795–802. <https://doi.org/10.1021/acs.jafc.9b07697>.

50. Su R, Yan H, Li P, et al. Photo-enhanced antibacterial activity of polydopamine-curcumin nanocomposites with excellent photodynamic and photothermal abilities. *Photodiagnosis Photodyn Ther.* 2021;35:1–11. <https://doi.org/10.1016/j.pdpdt.2021.102417>.
51. Zhao Z, Chen S, Xiao Y, et al. Supercritical fluid-assisted fabrication of PDA-coated poly (l-lactic acid)/curcumin microparticles for chemophotothermal therapy of osteosarcoma. *Coatings.* 2022;12:1–14. <https://doi.org/10.3390/COATINGS12040524>.
52. Lei L, Tu Q, Zhang X, et al. Stimulus-responsive curcumin-based polydopamine nanoparticles for targeting Parkinson's disease by modulating α -synuclein aggregation and reactive oxygen species. *Chem Eng J.* 2023. <https://doi.org/10.1016/j.cej.2023.141606>.
53. Stierli S, Napoli I, White IJ, et al. The regulation of the homeostasis and regeneration of peripheral nerve is distinct from the CNS and independent of a stem cell population. *Development (Cambridge).* 2018. <https://doi.org/10.1242/DEV.170316/VIDEO-1>.
54. Stierli S, Imperatore V, Lloyd AC. Schwann cell plasticity-roles in tissue homeostasis, regeneration, and disease. *Glia.* 2019;67:2203–15. <https://doi.org/10.1002/GLIA.23643>.
55. Mauritz C, Grothe C, Haastert K. Comparative study of cell culture and purification methods to obtain highly enriched cultures of proliferating adult rat Schwann cells. *J Neurosci Res.* 2004;77:453–61. <https://doi.org/10.1002/jnr.20166>.
56. Mosmann T. Rapid colorimetric assay for cellular growth and survival: application to proliferation and cytotoxicity assays. *J Immunol Methods.* 1983;65:55–63. [https://doi.org/10.1016/0022-1759\(83\)90303-4](https://doi.org/10.1016/0022-1759(83)90303-4).
57. Souza TGF, Ciminelli VST, Mohallem NDS. A comparison of TEM and DLS methods to characterize size distribution of ceramic nanoparticles. *J Phys Conf Ser.* 2016;733:012039. <https://doi.org/10.1088/1742-6596/733/1/012039>.
58. Chatterjee P, Dutta SS, Chakraborty T. Tautomers and rotamers of curcumin: a combined UV spectroscopy, high-performance liquid chromatography, ion mobility mass spectrometry, and electronic structure theory study. *J Phys Chem A.* 2022;126:1591–604. <https://doi.org/10.1021/acs.jpca.1c08612>.
59. Mondal S, Ghosh S, Moulik SP. Stability of curcumin in different solvent and solution media: UV–visible and steady-state fluorescence spectral study. *J Photochem Photobiol B.* 2016;158:212–8. <https://doi.org/10.1016/j.jphotobiol.2016.03.004>.
60. Shen L, Ji HF. The pharmacology of curcumin: Is it the degradation products? *Trends Mol Med.* 2012;18:138–44.
61. Morita M, Prudent J, Basu K, et al. mTOR controls mitochondrial dynamics and cell survival via MTFP1. *Mol Cell.* 2017;67:922–935.e5. <https://doi.org/10.1016/j.molcel.2017.08.013>.
62. Thaloor D, Miller KJ, Gephart J, et al. Systemic administration of the NF- κ B inhibitor curcumin stimulates muscle regeneration after traumatic injury. *Am J Physiol Cell Physiol.* 1999;277:C320–9. <https://doi.org/10.1152/ajpcell.1999.277.2.c320>.

Publisher's Note Springer Nature remains neutral with regard to jurisdictional claims in published maps and institutional affiliations.